May 1999

ELSEVIER

Materials Letters 39 (1999) 221–226

MATERIALS LETTERS

www.elsevier.com/locate/matlet

Phase stability of (Y,NB)-TZP/Al_2O_3 composites under low temperature hydrothermal conditions

Deuk Yong Lee [a,*], Dae-Joon Kim [b], Joo-Wung Jang [b], Dae-Weon Choi [c], Seung-Jae Lee [d]

[a] *Department of Metallurgical and Materials Engineering, Daelim College of Technology, Anyang 431-715, South Korea*
[b] *Ceramics Division, Korea Institute of Science and Technology, Seoul 136-791, South Korea*
[c] *Department of Ceramic Engineering, Yonsei University, Seoul 120-749, South Korea*
[d] *Department of PWR Fuel Development, Korea Nuclear Fuel, Taejeon 305-353, South Korea*

Received 14 August 1998; received in revised form 5 November 1998; accepted 7 December 1998

Abstract

Y_2O_3 and Nb_2O_5 co-doped tetragonal zirconia polycrystals (TZP) containing 10 to 30 vol.% Al_2O_3 ((Y,Nb)-TZP/Al_2O_3) were sintered for 5 h at 1550°C in air and hydrothermal stability of the composites was evaluated after aging for 5 h at 180°C in 0.3 MPa H_2O vapor pressure. (Y,Nb)-TZP/Al_2O_3 composites showed superior phase stability under the hydrothermal condition as compared with 3Y-TZP/Al_2O_3 composites due to the effects of Y–Nb ordering in t-ZrO_2 and the Al_2O_3 addition. The optimized strength and fracture toughness were 670 MPa and 7.3 MPa $m^{1/2}$, respectively, when 20 vol.% of 2.8 μm Al_2O_3 particles were added.

Keywords: Tetragonal zirconia polycrystals; Y_2O_3 and Nb_2O_5 co-doped zirconia/Al_2O_3 composite; Hydrothermal stability; Mechanical properties

1. Introduction

Although yttria-stabilized tetragonal zirconia polycrystals (Y-TZPs) possess high strength and toughness at room temperature, they suffer low-temperature strength degradation (LTD) because of the spontaneous tetragonal (t) to monoclinic (m) phase transformation when annealed at temperatures from 100 to 500°C in air. The LTD is accelerated under hydrothermal environments [1–3]. The phase stability of TZP under the hydrothermal conditions is a critical requirement for applications of TZP for use in medical devices such as the femoral head in total hip replacement, dental implants, and scalpels. Attempts to alleviate LTD of Y-TZP through a decrease in grain size, an increase in yttrium content, and the formation of composites with Al_2O_3 have been tried [3–8].

Considerable efforts have been exerted to elucidate the mechanism of hydrothermal degradation in Y-TZP. The yttrium depletion by $Y(OH)_3$ formation in the presence of water vapor by Lange et al. [2] was proposed as the cause of the aging-induced degradation. Yoshimura [9] suggested that the hy-

* Corresponding author

00167-577X/99/$ - see front matter
PII: S0167-577X(99)00010-5

drothermal degradation of Y-TZP is controlled by OH^- diffusion rather than $Y(OH)_3$ formation. Kim et al. [10–12] reported that LTD of Y-TZP is governed not by the existence of H_2O but the amount of residual stress in t-ZrO_2 during aging, which is accumulated by the diffusion of oxygen vacancies. The residual stress facilitates the t → m phase transformation and the reaction between Zr–O–Zr bond and H_2O.

Recently, Lee et al. [13] examined the t-phase stability composition region in the ZrO_2–Y_2O_3–Nb_2O_5 system and showed that Nb_2O_5 doping to Y-TZP ((Y,Nb)-TZP) influenced remarkably the fracture toughness and LTD. The phase stability of TZPs in the ternary system is likely due to the Y–Nb ordering in t-ZrO_2 lattice [14]. The addition of Al_2O_3 into Y-TZP enhanced fracture strength and phase stability because Al_2O_3 particles acted as a grain-growth inhibitor for Y-TZP [15–17]. In particular, 2 to 3.85 mol% Y-TZP, alloyed with 20 to 40 wt.% Al_2O_3 and prepared by hot isostatic pressing, exhibited extremely high strength of above 2 GPa [16], fracture toughness of 17 MPa $m^{1/2}$ [15], and high temperature strength of 1 GPa at 1000°C [17]. Nevertheless, about 25% of t-ZrO_2 transformed to m-ZrO_2 during aging for 5 h at 180°C in an autoclave [18]. Although hydrothermal stability was improved by alloying with CeO_2, the (Y,Ce)-TZP/Al_2O_3 composites exhibited about 10% of m-ZrO_2 after aging for 5 h at 180°C in hot water [18].

The objective of the present study is to investigate the hydrothermal stability of (Y,Nb)-TZP/Al_2O_3 composites containing 10 to 30 vol.% of Al_2O_3 and to compare with that of 3Y-TZP/Al_2O_3 composites after aging at 180°C for 5 h in an autoclave.

2. Experimental procedure

The powder preparation procedure of (Y,Nb)-TZP having a composition of 90.31 mol% ZrO_2—5.31 mol% Y_2O_3—4.45 mol% Nb_2O_5 was reported elsewhere [13]. The starting powders, (Y,Nb)-TZP, 3Y-TZP (Tosoh, Japan), and Al_2O_3 (Sumitomo Chemical, Japan) with different average particle sizes (0.2 and 2.8 μm), were ball milled for 24 h using zirconia balls. The amount of powders was measured on the basis of the theoretical densities of 6.02, 6.08, and 3.99 for (Y,Nb)-TZP, 3Y-TZP, and Al_2O_3, respectively. Al_2O_3 particles (0.2 and 2.8 μm) were mixed to (Y,Nb)-TZP and 3Y-TZP by 10 vol.% intervals in the range of 10 to 30 vol.%. The resulting composites are designated as YN10$f(c)$, YN20$f(c)$, YN30$f(c)$, 3Y10$f(c)$, 3Y20$f(c)$, and 3Y30$f(c)$, respectively. The last digit, f and c, indicates the Al_2O_3 particle size, 0.2 μm and 2.8 μm, respectively.

The powders were uniaxially pressed into 34 mm × 34 mm × 5 mm rectangular plates at 98 MPa and then isostatically pressed at 138 MPa. The specimens were sintered at 1550°C with heating rates of 6°C/min to 900°C and 3°C/min up to the sintering temperature, and then furnace cooled to room temperature. The sintered specimens were ground and polished down to 1 μm diamond finish.

The bulk density of (Y,Nb)-TZP/Al_2O_3 and 3Y-TZP/Al_2O_3 composites was determined by the Archimedes method. The samples were aged for 1000 h at 250°C in air or for 5 h at 180°C in 0.3 MPa water vapor pressure in an autoclave. Phase stability of t-ZrO_2 after aging was studied using X-ray diffractometry. The proportion of the t and m-phase was estimated from the X-ray diffraction (XRD) peak heights of $(111)_m$, $(11\text{-}1)_m$, and $(111)_t$ after Garvie and Nicholson [19]. XRD patterns were obtained from the Cuκα radiation at 40 kV and 30 mA within the scan angles (2θ) of 27° to 35°. The linear intercept method was used to determine the average grain size with the use of a correction factor of 1.56 after Mendelson [20].

The rectangular specimens were ground and cut with diamond saw to a size of 24 mm × 4 mm × 3 mm, and subsequently annealed for 1 h at 1200°C. The flexural strength was measured using a 3-point bending with a 20 mm outer span at a crosshead speed (Instron 4204) of 0.5 mm/min. Fracture toughness of bar specimens was then assessed using the indentation/strength method [21]. A Vickers indent of 294 N was placed on the center of the tensile face of each test piece by aligning the pyramidal edges to the longitudinal axis for the bar specimens. To prevent the stress-corrosion cracking, a silicon oil was dropped on the indented site and then specimens were broken using a 4-point bending fixture. The hardness-to-modulus ratio (H/E) was determined by measuring the dimensions of the Knoop indentation

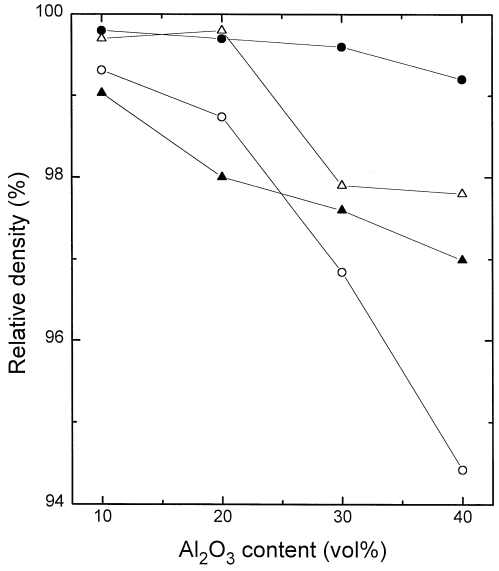

Fig. 1. Relative density of 3Y-TZP/Al_2O_3 and (Y,Nb)-TZP/Al_2O_3 composites having different Al_2O_3 particle sizes, where the specimens were sintered for 5 h at 1550°C in air. ● (Y,Nb)-TZP/2.8 μm Al_2O_3; ▲ (Y,Nb)-TZP/0.2 μm Al_2O_3; ○ 3Y-TZP/2.8 μm Al_2O_3; △ 3Y-TZP/0.2 μm Al_2O_3.

impression dimensions as reported by Marshall et al. [22].

3. Results and discussion

The relative density of the composites, sintered for 5 h at 1550°C in air, is shown in Fig. 1. The relative density of YN10*c* rose from 97.8% to 99.8% as the sintering time increased from 1 h to 5 h. This is consistent with the densification behavior of 3Y-TZP/Al_2O_3 reported by Upadhyaya et al. [23]. The relative density of all composites decreased as the content of Al_2O_3 increased from 10 to 40%. The reduction in the density may be ascribed to a reduced grain boundary mobility of the zirconia matrix with increasing ratio of Al_2O_3 reinforcement as a result of limited interdiffusion caused by an increase in the diffusion path lengths [23].

The grain size and m-ZrO_2 content of 3Y-TZP and (Y,Nb)-TZP are summarized in Table 1. All specimens showed t-ZrO_2 phase only after sintering for 5 h at 1550°C in air. When 3Y-TZP was annealed for 1000 h at 250°C in air, XRD results revealed that about 65% of the t-ZrO_2 phase transformed to m-ZrO_2 even though the grain size of 3Y-TZP, 0.7 μm, was much smaller than that of (Y,Nb)-TZP shown in Table 1. The beneficial effect of the Nb_2O_5 alloying into Y-TZP on its aging resistance is clearly seen from Table 1 where no m-ZrO_2 phase was observed on (Y,Nb)-TZP after aging in air or in an autoclave. The absence of the degradation in (Y,Nb)-TZP under the low-temperature conditions is attributed to local Y–Nb ordering in t-ZrO_2 into a scheelite-like arrangement [13,14], which results in a relief of the internal strain in the t-ZrO_2 lattice since the internal stress causes the degradation [10–12]. Furthermore, the concentration of oxygen vacancy in t-ZrO_2, created by the Y^{3+} doping, decreased by the addition of Nb^{5+}, leading to a low vacancy diffusion rate which governed the t → m phase transformation during aging at low temperatures [11,12].

After aging in air and in water vapor, XRD analysis of the aged composites showed that the amount of m-ZrO_2 decreased with increasing Al_2O_3 content, as shown in Fig. 2. The decrease in m-ZrO_2 by the addition of Al_2O_3 is likely achieved by hindering a relaxation of the strained t-ZrO_2 lattice due to the presence of the rigid Al_2O_3 particles. The m-ZrO_2 content of 3Y10*f* was 24% after aging in air. The degree of t → m phase transformation increased significantly from 24% to 70% when 3Y10*f* was exposed to aging in the autoclave since the high pressure aging condition accelerates the relaxation [11]. The addition of 2.8 μm Al_2O_3 into 3Y-TZP raised the amount of m-ZrO_2 almost close to 3Y-TZP

Table 1
Grain size and m-ZrO_2 content of 3Y-TZP and (Y,Nb)-TZP sintered for 5 h at 1550°C in air

Sample	Grain size (μm)	m-ZrO_2 (%), aging in air	m-ZrO_2 (%), aging in autoclave
3Y-TZP	0.7	65	87
(Y,Nb)-TZP	2.4	0	0

Specimens are aged for 1000 h at 250°C in air or for 5 h at 180°C in 0.3 MPa water vapor pressure.

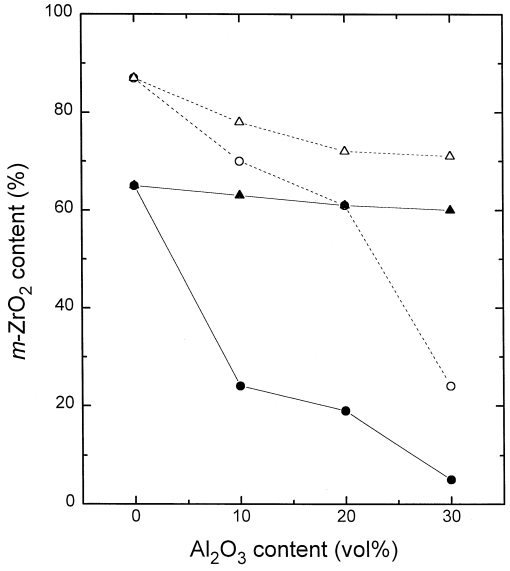

Fig. 2. Fraction of *m*-ZrO_2 of the aged surfaces of 3Y-TZP/Al_2O_3 and (Y,Nb)-TZP/Al_2O_3 composites as a function of Al_2O_3 content, where the specimens were sintered at 1550°C for 5 h and aging was performed for 1000 h at 250°C in air or for 5 h at 180°C in 0.3 MPa H_2O vapor pressure. ● 3Y-TZP/0.2 μm Al_2O_3 in air; ▲ 3Y-TZP/2.8 μm Al_2O_3 in air; ○ 3Y-TZP/0.2 μm Al_2O_3 in autoclave; △ 3Y-TZP/2.8 μm Al_2O_3 in autoclave.

after aging as shown in Fig. 2, indicating that the larger Al_2O_3 particles were little influential in the phase stability of the composites probably due to the large grain size. In contrast, there was no degradation in (Y,Nb)-TZP regardless of the Al_2O_3 content owing to the inherent phase stability of t-ZrO_2 in this composition [13].

Flexural strength and fracture toughness of (Y,Nb)-TZP/Al_2O_3 composites containing 0 to 30 vol.% Al_2O_3 are shown in Fig. 3. The flexural strength of (Y,Nb)-TZP/Al_2O_3 composites increased as Al_2O_3 was added up to 20 vol.% and then decreased with further addition of Al_2O_3, which is consistent with the results reported earlier [16,23,24]. This reduction in strength above 20 vol.% of Al_2O_3 may be explained by decrease in constraint on the t-ZrO_2 as a result of the low bulk density [24]. Although flexural strength of YN20*f* was slightly higher than that of YN20*c*, the optimized strength and fracture toughness, 670 MPa and 7.3 MPa $m^{1/2}$, were observed when 20 vol.% of 2.8 μm Al_2O_3 particles were added. SEM micrographs of (Y,Nb)-TZP/Al_2O_3 composites containing 10 to 30 vol.% of 2.8 μm Al_2O_3 are shown in Fig. 4. The white and the black grains indicate ZrO_2 grains and Al_2O_3 grains, respectively. The grain size of ZrO_2 in the (Y,Nb)-TZP/Al_2O_3 composites was smaller than that in monolithic (Y,Nb)-TZP [13], indicating the role of Al_2O_3 as a grain growth inhibitor.

XRD results of the fracture surfaces of (Y,Nb)-TZP/Al_2O_3 and 3Y-TZP/Al_2O_3 composites are shown in Fig. 5 as a function of Al_2O_3 content. In both composites, the fraction of m-ZrO_2 decreased with increasing the amounts of Al_2O_3. However, the decreasing rate of m-ZrO_2 in the composites having 0.2 μm Al_2O_3 particles is more pronounced compared with that in the composites having 2.8 μm Al_2O_3 particles, indicating that the influence of the stress-induced phase transformation on mechanical properties of the composites is lessened with increased Al_2O_3 contents and decreased Al_2O_3 particle size due to the decrease in transformable t-ZrO_2 content. Nevertheless, (Y,Nb)-TZP/Al_2O_3 composites showed the optimized fracture toughness of 7.3 MPa $m^{1/2}$ and 6.4 MPa $m^{1/2}$, respectively, when 20

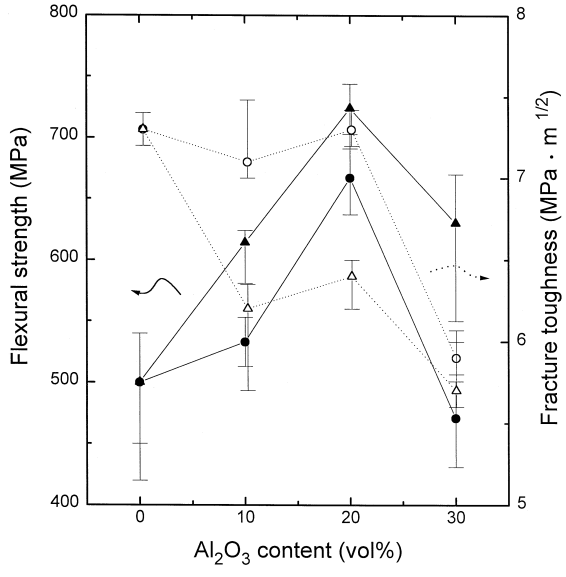

Fig. 3. Flexural strength and fracture toughness of (Y,Nb)-TZP/Al_2O_3 composites, prepared by sintering for 5 h at 1550°C in air, as a function of Al_2O_3 content. ● (Y,Nb)-TZP/2.8 μm Al_2O_3; ▲ (Y,Nb)-TZP/0.2 μm Al_2O_3; ○ (Y,Nb)-TZP/2.8 μm Al_2O_3; △ (Y,Nb)-TZP/0.2 μm Al_2O_3.

vol.% of 2.8 μm and 0.2 μm Al_2O_3 particles were added, as shown in Fig. 3. The highest fracture

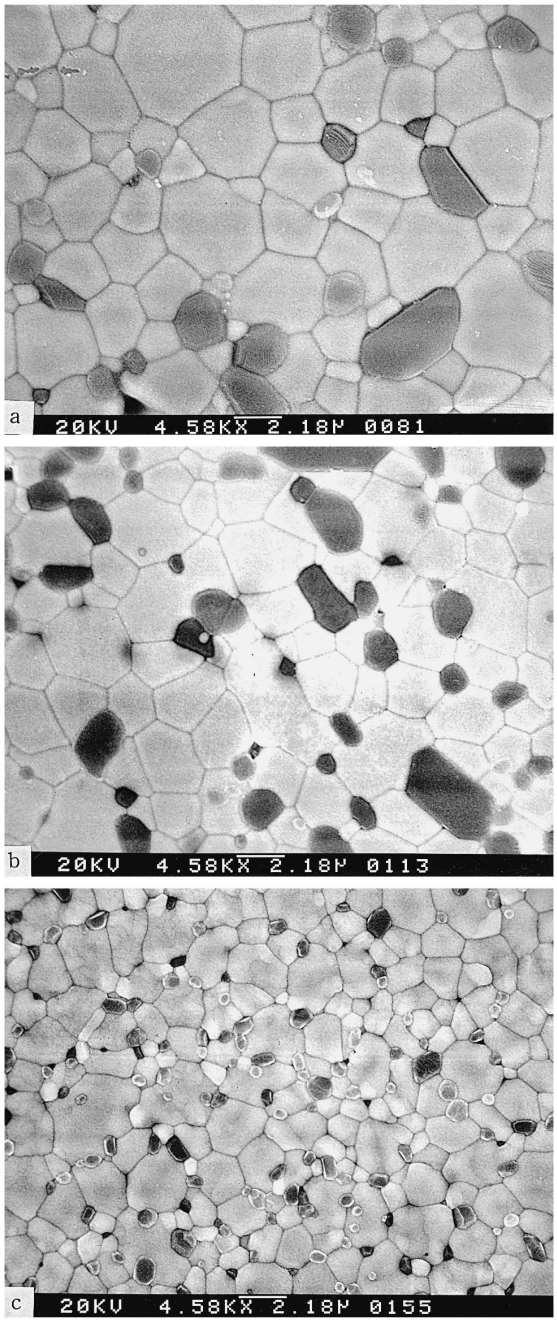

Fig. 4. Scanning electron micrographs of the thermally etched surface of (Y,Nb)-TZP/2.8 μm Al_2O_3 composites after sintering for 5 h at 1550°C in air. (a) 10 vol.% of Al_2O_3; (b) 20 vol.%; (c) 30 vol.%.

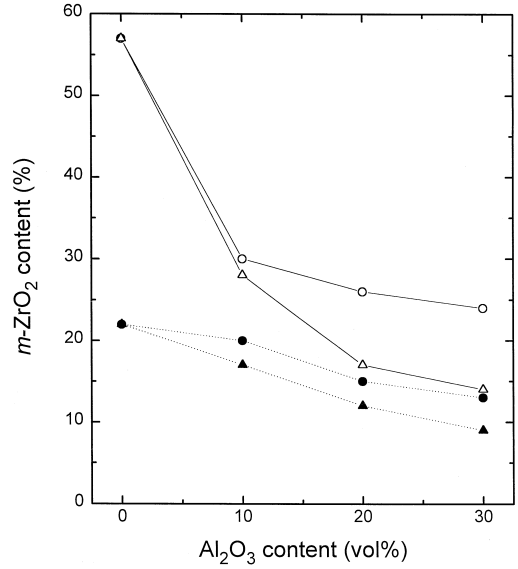

Fig. 5. Fraction of m-ZrO_2 on the fracture surfaces of 3Y-TZP/Al_2O_3 and (Y,Nb)-TZP/Al_2O_3 composites, sintered at 1550°C for 5 h in air, as a function of Al_2O_3 content. ● 3Y-TZP/2.8 μm Al_2O_3; ▲ 3Y-TZP/0.2 μm Al_2O_3; ○ (Y,Nb)-TZP/2.8 μm Al_2O_3; △ (Y,Nb)-TZP/0.2 μm Al_2O_3.

toughness at these composition indicates that the fracture toughness strongly depends on the strength according to the Griffith relationship [25]. And the toughness difference between YN20*c* and YN20*f* may be ascribed to the contribution of transformation toughening and the grain bridging due to the Al_2O_3 particle size [26]. Therefore, the Al_2O_3 particle with larger size was more effective to increase fracture toughness of the composites with the same Al_2O_3 content.

4. Conclusions

No hydrothermal degradation was observed on (Y,Nb)-TZP/Al_2O_3 composites after aging for 5 h at 180°C and 0.3 MPa in an autoclave, however, extensive t → m phase transformation was found in 3Y-TZP/Al_2O_3 composites. The m-ZrO_2 content of the aged 3Y-TZP/Al_2O_3 composites decreased with increasing Al_2O_3 content due to the stability of t-ZrO_2 caused by the addition of Al_2O_3. Therefore, the Nb_2O_5 doping to Y-TZP is more effective to the phase stability than Al_2O_3 alloying into Y-TZP.

The optimized strength and fracture toughness of (Y,Nb)-TZP/Al_2O_3 composite, sintered for 5 h at 1550°C in air, were 670 MPa and 7.3 MPa $m^{1/2}$, respectively when 20 vol.% of 2.8 μm Al_2O_3 was added. Fracture toughness increase was better in the composite dispersed with Al_2O_3 particle of larger size.

References

[1] T. Sato, M. Shimada, J. Am. Ceram. Soc. 68 (6) (1985) 356.
[2] F.F. Lange, G.L. Dunlop, B.I. Davis, J. Am. Ceram. Soc. 69 (3) (1986) 237.
[3] S. Lawson, J. Eur. Ceram. Soc. 15 (1995) 485.
[4] S.Y. Chen, H.Y. Lu, J. Mater. Sci. 23 (1988) 1195.
[5] D. Basu, A. Das Gupta, M.K. Basu, B.K. Sarkar, J. Eur. Ceram. Soc. 16 (1996) 613.
[6] M.M.R. Boutz, A.J.A. Winnubst, B. Van Langerak, R.J.M. Olde Scholtenhuis, K. Kreuwel, A.J. Burggraaf, J. Mater. Sci. 30 (1995) 1854.
[7] A.E. Hughes, H. St. John, P. Koutouros, H. Schubert, J. Eur. Ceram. Soc. 15 (1995) 1125.
[8] M.T. Hernandez, J.R. Jurado, P. Duran, J.L.G. Fierro, J. Am. Ceram. Soc. 74 (1991) 1254.
[9] M. Yoshimura, Am. Ceram. Soc. Bull. 67 (12) (1988) 1950.
[10] D.-J. Kim, H.-J. Jung, D.-H. Cho, Solid State Inonics 80 (1995) 67.
[11] D.-J. Kim, J. Eur. Ceram. Soc. 17 (1997) 897.
[12] D.-J. Kim, H.-J. Jung, J.-W. Jang, H.-L. Lee, J. Am. Ceram. Soc., in press.
[13] D.Y. Lee, D.-J. Kim, D.-H. Cho, J. Mater. Sci. Lett. 17 (1998) 185.
[14] P. Li, I.-W. Chen, J.E. Penner-Hahn, J. Am. Ceram. Soc. 77 (1994) 1289.
[15] J. Li, R. Watanabe, J. Am. Ceram. Soc. 78 (1995) 1079.
[16] K. Tsukuma, K. Ueda, M. Shimada, J. Am. Ceram. Soc. 68 (1985) C4.
[17] K. Tsukuma, K. Ueda, K. Matsushita, M. Shimada, J. Am. Ceram. Soc. 68 (1985) C56.
[18] M. Hirano, H. Inada, J. Ceram. Soc. Jpn. 99 (1991) 124.
[19] R.C. Garvie, P.S. Nicholson, J. Am. Ceram. Soc. 55 (1972) 303.
[20] M.J. Mendelson, J. Am. Ceram. Soc. 52 (1969) 443.
[21] P. Chantikul, G.R. Anstis, B.R. Lawn, D.B. Marshall, J. Am. Ceram. Soc. 64 (1981) 539.
[22] D.B. Marshall, T. Noma, A.G. Evans, Commun. Am. Ceram. Soc. 65 (1982) C–175.
[23] D.D. Upadhyaya, P.Y. Lalvi, G.K. Dey, J. Mater. Sci. 28 (1993) 6103.
[24] J.L. Shi, B.S. Li, T.S. Yen, J. Mater. Sci. 28 (1993) 4019.
[25] B. Lawn, Fracture of Brittle Solids, 2nd ed. Cambridge Univ. Press, Cambridge, UK, 1993.
[26] D.Y. Lee, D.-J. Kim, J. Am. Ceram. Soc., to be submitted.